Journal Article

Control of the properties of xanthan / glucomannan mixed gels by varying xanthan fine structure

Fitzpatrick, P., Meadows, J., Ratcliffe, I. and Williams, P.A.

Control of the properties of xanthan/glucomannan mixed gels by varying xanthan fine structure

P. Fitzpatrick*, J. Meadows,** I. Ratcliffe, Peter A. Williams+,

Centre for Water Soluble Polymers, Glyndwr University, Plas Coch, Mold Road, Wrexham, LL11 2AW, UK

Key words

Konjac glucomannan, xanthan gum, thermoreversible gels, DSC, coil-helix transition

+ corresponding author: Professor Peter A. Williams, Centre for Water Soluble Polymers, Glyndwr University, Plas Coch, Mold Road, Wrexham, LL11 2AW, UK

email: williamspa@glyndwr.ac.uk

.....

*present address: C-Tech Innovation Ltd, Capenhurst Technology Park, Chester, CH1 6EH, United Kingdom. Email: paul.fitzpatrick@ctechinnovation.com

** present address: IS Pharmaceuticals Ltd , Office Village , Chester Business Park , Chester CH4 9QZ , United Kingdom. Email: jmeadows@sinclairpharma.com

Abstract

The interaction of native xanthan gum, deacetylated xanthan gum and depyruvated xanthan gum with konjac glucomannan has been studied using DSC and controlled stress rheometry. In the absence of electrolyte the DSC cooling curves for native xanthan and deacetylated xanthan showed a single peak and there was a corresponding sharp increase in the storage modulus indicating gel formation. It is apparent that on cooling, association of the konjac glucomannan with the native xanthan molecules is triggered by the xanthan coil-helix transition. In the presence of electrolyte, there were two DSC peaks observed. The higher temperature DSC peak was attributed to the xanthan coil-helix transition while the lower temperature DSC peak was attributed to konjac glucomannan – xanthan association as noted by an increase in the storage modulus. The gels formed were much weaker than those in the absence of electrolyte. The DSC cooling curves for depyruvated xanthan in the absence of electrolyte showed two peaks. The higher temperature peak was attributed to the coil-helix transition while the lower temperature peak corresponded to gelation as noted by an increase in the storage modulus. The gels were very much weaker than for native xanthan gum and deacetylated xanthan gum.

Introduction

Xanthan gum is an exocellular polysaccharide produced by the bacterium *Xanthomonas campestris* and is nowadays very widely used in a broad range of products, including foods, pharmaceuticals, cosmetics, personal care, drilling muds etc. because of its unique rheological properties (Sworn, 2009: Morris, 2006). Essentially, xanthan gum solutions exhibit a very high viscosity at low shear rates because of weak intermolecular association of the polysaccharide chains. However, the solutions are very shear thinning since the weak intermolecular associations are readily disrupted. The gum is, therefore, widely used to stabilise dispersions and emulsions because of its ability to inhibit particle sedimentation and droplet creaming (Velez, Fernandez, Munoz & Williams, 2003). Xanthan molecules consist of a main chain of (1,4) β – D- glucose residues with a trisaccharide side chain attached to every other glucose. The side chains are linked through the 3 position and consist of β - D – mannose (1,4) – β - D - glucuronic acid (1,2) α- D – mannose. The inner mannose may be acetylated and the terminal mannose may be pyruvated. Xanthan molecules have been shown by X-Ray fibre diffraction studies to adopt a right-handed helical conformation with five-fold symmetry and a pitch of 4.7nm (Moorhouse, Walkinshaw & Arnott, 1977). It has been clearly demonstrated by a range of techniques including, optical rotation, viscosity, light scattering, electron microscopy, DSC, NMR and ESR, that the molecules undergo a conformational transition in solution to form a more flexible disordered state which is favoured at increasing temperature and low ionic strength (Norton et al 1984: Milas & Rinaudo 1986: Lui & Norisuye, 1988: Foss, Stokke & Smidsrød, 1987: Gamini, de Bleijser & Leyte, 1991: Takigami, Shimada, Williams & Phillips, 1993). There is much controversy reported in the literature as to whether the molecules adopt single helices, double helices or dimers through association of single helical chains in solution. For example, Norton et al (1984) argued that the molecules adopt a single helical conformation with the side chains packed along the backbone and that ordered and disordered sequences may co-exist within

the same molecule. Milas and Rinaudo (1986) also favoured the single helix model and suggested that the molecules can adopt three distinct molecular conformations. In the native state, the molecules are completely ordered and on heating become completely disordered. On further cooling the molecules order but are more expanded than the native state as a consequence of different side chain – backbone interactions. On the other hand Lui et al (1988) concluded that the ordered structure was a double helix and that on increasing the temperature the molecules unwind from both ends forming an expanded dimer joined by a short helical section. Foss et al (1987) produced electron micrographs showing that the ordered xanthan consists of two associated molecules with sections of single strands at one or both ends. NMR studies by Gamini et al (1991) provided support for the expanded dimer concept and also indicated that on heating considerable side chain mobility is established before any significant increase in the mobility of the backbone is observed. In the ordered form the side chains are associated with the cellulosic backbone thus stabilising the helical structure, while in the disordered form there is no association with the backbone and the side chains are free to rotate. Further confirmation of the involvement of the side chains in the ordering process has been provided through ESR studies by Takigami et al (1993) using nitroxide spin labels attached to the carboxylate groups in the side chains. At high temperatures the side chains were found to be highly mobile giving rise to isotropic ESR spectra but on cooling to temperatures below the conformational transition, anisotropic spectra were obtained indicating a significant loss of mobility. The temperature of the conformational transition is dependent on the amount of acetyl and pyruvate groups present (Shatwell, Sutherland, Dea & Ross-Murphy, 1990: Cheetham & Mashimaba, 1992: Callet, Milas & Rinaudo, 1987). It has been shown that it shifts to lower temperatures by removal of acetyl groups but increases to higher temperatures on removal of pyruvate groups. The acetyl groups on the side chains are able to interact with the cellulosic backbone through hydrogen or hydrophobic bonding thus promoting the ordered structure. The destabilising effect of the pyruvate groups has been attributed to the increase in electrostatic charge repulsion as a result of the side chains folding in on the backbone.

94 It is well known that xanthan gum will form thermoreversible gels in the presence of certain
95 galactomannans, namely locust bean gum and tara gum and also with glucomannans
96 (konjac mannan) (Cheetham & Mashimba, 1992: Dea et al, 1977: Callet, Milas & Rinaudo,
97 1987: Dea & Morrison 1975: Williams et al 1991a: Williams et al 1991b: Williams & Phillips
98 1995: Annable, Williams & Nishinari, 1994: Fitzsimons, Tobin & Morris, 2008: Abbaszadeh &
99 Foster, 2012: Wielinga, 2009). The galactomannans consist of linear chains of β (1,4)
100 mannose residues with galactose residues linked at the 6 position (Takigami, 2009). The
101 mannose to galactose ratio is 3:1 for tara gum and 4:1 for locust bean gum. Glucomannans
102 consist of linear chains of β (1,4) glucose and mannose residues with branches consisting of
103 up to 16 sugar units linked to the 3 position on the main chain (Nishinari, Williams & Phillips
104 1992). There is approximately one branch every 10 residues along the chain. The mannose
105 to glucose ratio is 1.6:1. The molecules also contain acetyl groups (approximately 1 per 17
106 sugar residues). A common feature of galactomannans and glucomannans with respect to
107 their interaction with xanthan gum is that they adopt an extended conformation in solution.
108 The thermoreversible gels formed by mixing xanthan gum with tara gum, locust bean gum or
109 konjac glucomannan are optically clear and highly elastic and have considerable commercial
110 importance. The mechanism of the gelation process has been a matter of much controversy
111 and a detailed review has been published previously (Williams & Phillips, 1995). It is clear
112 that the main body of evidence indicates that gelation occurs as a consequence of the
113 molecular association of xanthan molecules with galacto- and gluco- mannan chains.
114 Brownsey et al (1988) studied the mixed systems using X-Ray diffraction and the X-Ray fibre
115 pattern obtained provided direct evidence of intermolecular binding. Since gels were only
116 formed when solutions were mixed at temperatures above the xanthan coil-helix transition,
117 binding was assumed to involve the disordered xanthan chains. Dea and Morrison (1975),
118 however, proposed that association involved the ordered xanthan helices. More recent work
119 by Fitzsimons et al (2008) provides further evidence that the association does not require
120 xanthan to be in the disordered form. These workers, however, demonstrated that stronger

121 gels are formed after heating to 95°C [i.e.above the temperature of the coil helix transition]
122 and then cooling to 20°C than those obtained on mixing at 20°C. This is in agreement with
123 our own previous work using a combination of DSC, rheology and ESR techniques which
124 demonstrated that the molecular association between xanthan and galacto- and gluco-
125 mannans only occurs at temperatures at or below the xanthan conformational transition
126 (Williams et al 1991b: Williams & Phillips, 1995: Annable, Williams & Nishinari, 1994). A
127 number of workers (Abbaszadeh & Foster 2012: Tako, Asato & Nakamura, 1984: Shatwell,
128 Sutherland, Ross-Murphy & Dea, 1991) have shown that the interaction of xanthan with
129 galacto- and gluco- mannans is dependent of the degree of acetylation and pyruvation of the
130 xanthan molecules. Deacetylated xanthan has been found to produce much stronger gels
131 than native or depyruvated xanthan molecules. This study sets out to gain a further insight
132 into the mechanism of gelation of konjac glucomannan / xanthan gum mixed systems using
133 xanthan, deaceylated xanthan and depyruvated xanthan with a view to controlling the
134 thermal and rheological properties of the mixed gels.

135

136 **Materials and Methods**

137 *Xanthan gum*

138 A commercial sample of xanthan gum was dialysed against deionised water and the metal
139 ion content determined using Atomic Absorption. It was found to contain 0.021% Na, 0.029%
140 K and 0.002% Ca. The acetyl content was determined by alkaline hydrolysis as follows:
141 Nitrogen gas was passed through 100mL 0.5% w/w xanthan solution for 10 min and 3mL of
142 1M KOH added. The flask was stoppered and left for 2 days at room temperature was
143 intermittent stirring. 30mL 0.05 H_2SO_4 was added and the excess acid was titrated with
144 0.01M KOH using phenolphthalein indicator. It was found that 93% of the side chains were
145 acetylated. The pyruvate content was determined using the method reported by Sloneker

146 and Orentas (1962) and it was found that 25% of the side chains contained a pyruvate
147 group.
148
149 *Deacetylated xanthan gum*
150 The commercial sample reported above was deacetylated using the method described by
151 Tako & Nakamura, (1984).
152
153 *Depyruvated xanthan gum*
154 A sample of depyruvated xanthan was provided as a gift and it was found that 90% of the
155 side chains were acetylated and 7% contained a pyruvate group.
156
157 *Konjac glucomannan (KM)*
158 A commercial sample of hydroprocessed konjac glucomannan was obtained and was used
159 as received. It was found to contain negligible amounts of metal ions and had a molecular
160 mass of 480KDa and acetyl content of 1 per 17 sugar units.
161
162 *Differential scanning calorimetry*
163 Measurements were performed using a Seteram micro DSC fitted with 1mL sample vessels.
164 The polymer solution was accurately weighed into the sample cell and the reference cell was
165 filled with the same weight of solvent. Instrumental baselines were determined with both the
166 sample and reference cells filled with solvent and the curve produced was subtracted from
167 the sample curve. The scans were determined at a scan rate of 0.2°C per minute and an
168 initial heat / cool cycle was undertaken to ensure the same thermal history.
169
170 *Rheological measurements*
171 Rheological experiments were performed on a Carrimed CSL 100 Controlled Stress
172 Rheometer using cone and plate geometry (2 degree x 5 cm). Samples were prepared in the
173 presence and absence of electrolyte and heated to 75°C then loaded onto the instrument.

They were then cooled at a constant rate of 1 °C /min in 5 °C steps. The storage (G') and loss (G") moduli were determined at each step at a frequency of 1Hz down to 15 °C. A 3 min equilibration step was allowed at each interval.

Results and Discussion

Xanthan conformational transition

The DSC cooling curves for native xanthan gum solutions (1.2% w/w) at different ionic strengths are given in Figure 1. The cooling curve in the absence of electrolyte (curve a) shows a very broad exothermic peak between ~35°-55°C which is not readily discernible. This indicates that the conformational transition occurs over a large temperature range and has a very small enthalpy. This is presumably due to the fact the charged carboxylate groups present on the xanthan side chains inhibit them from folding onto the xanthan backbone due to electrostatic repulsions and hence the molecules adopt a less ordered structure. In the presence of 5mM NaCl (curve b) a small exothermic peak is observed with a midpoint transition temperature, Tm, of 52.1°C which is attributed to the xanthan coil-helix transition. As the ionic strength is increased (curves c-g) the peak shifts to higher temperatures and becomes much sharper. The presence of the electrolyte will screen electrostatic repulsions between the charged groups on the side-chains enabling them to fold in and bind to the xanthan backbone and stabilise the helical structure. The xanthan molecules, therefore, undergo the coil-helix transition at a higher temperature and the molecules have a greater degree of order. The values for the midpoint transition temperature, Tm, and the enthalpy of the process, ΔH, are summarised in Table 1. It is noted that the enthalpy increases from -2.6 J/g in 1 mM NaCl up to -6.5 J/g in 20 mM NaCl and then remains constant. This latter value is in good agreement with Fitzsimons et al [21] who reported a value of – 6.00 J/g in 30mM KCl. Kitamura et al [30] also showed that ΔH was

independent of electrolyte concentration above 20mM NaCl but the actual value obtained was slightly higher than for our sample (8.6 J/g).

The corresponding DSC cooling curves for deacetylated xanthan gum solutions (1.2% w/w) at different ionic strengths are presented in Figure 2. It is evident that the conformational transition occurs at a lower temperature compared to xanthan itself at the various ionic strengths. The Tm values of the transition and the ΔH values are summarised in Table 1. The ΔH values follow a similar trend as for the standard xanthan sample in that they increase up to 20mM NaCl and then remain constant. However, the actual values (-4.2 J/g) are considerably lower for the deacetylated sample compared to the native xanthan. Presumably, the lower ΔH and Tm values are a consequence of the fact that when acetyl groups are removed from the mannose residues on the side chains, the side chains are no longer able to associate with the backbone as effectively and, therefore, are not able to stabilise the helical structure. Hence, lower temperatures are required for the coil-helix transition to occur and the molecules adopt a less ordered structure.

According to the Manning theory for polyelectrolytes (Manning, 1969a: Manning, 1969b: Manning 1996), counterion condensation will occur when the dimensionless linear charge density parameter, ξ , has a value greater than Z^{-1}, where Z is the valency of the counterion. ξ can be calculated using the relationship,

$$\xi = e^2 / 4 \pi \varepsilon_o \varepsilon \kappa T b \qquad \text{equation [1]}$$

where e, is electronic charge, ε_o and ε are the permittivity in vacuum and in the solvent, κ, is the Boltzmann constant, T, is the absolute temperature and b, is the spacing between charged groups along the polymer chain.

The fraction of polymer charges carrying a bound counterion, θ, is given by,

$$\theta = Z^{-1} [1 - 1/Z\xi] \qquad \text{equation [2]}$$

225 Norton et al (1984) carried out DSC studies on a sample of xanthan with an average of 0.67
226 pyruvate groups per side chain and, therefore, assumed an average of 1.67 charges per
227 xanthan pentasaccharide in order to calculate 'b'. This is perhaps an oversimplification of the
228 situation since the calculation should strictly have taken into account the distance between
229 the charged pyruvate and glucuronic acid groups on a single side chain and the distance
230 between charged groups on different side chains rather than the average. Nevertheless,
231 they calculated the distance of separation of the charges along the xanthan chain, b, to be
232 0.563nm for a single stranded chain and 0.281nm for a double stranded chain yielding
233 values for θ of 0.21 for a single helix and 0.61 for a double helix. The helix – coil transition,
234 therefore, should be accompanied by an increase in the degree of counterion condensation.
235 The extent of increased condensation can be determined using the relationship,

236 $$1/Tm = -\theta R \ln I / 2 \Delta H_c + \text{constant} \qquad \text{equation [3]}$$

237 where I is the ionic strength and ΔH_c is the enthalpy change per charge for helix melting.

238 The inverse transition midpoint temperatures for our samples are plotted as a function of the
239 natural logarithm of the ionic strength in Figure 3. The plots are linear as observed by other
240 workers (Norton et al, 1984: Abbaszadeh & Foster, 2012: Kitamura, Takeo, Kuge & Stokke,
241 1991) in agreement with predictions from equation [3]. The slope of the line was found to be
242 -0.22×10^{-3} and -0.20×10^{-3} for native xanthan and deacetylated xanthan respectively.
243 These values are close to the value of -0.17×10^{-3} reported by Norton et al (1984). They
244 used this value to calculate the change in the fraction of charged groups carrying a
245 condensed counterion, $\Delta\theta$, and obtained a value of 0.17. Not withstanding the comments
246 above, this value is close to the value of 0.12 predicted by Manning theory for a coil to single
247 helix transition and significantly less than the value of 0.52 for double helix formation.

248 Experiments were also undertaken using depyruvated xanthan gum in water and 40mM
249 NaCl and the DSC cooling curves are presented in Figure 4. A small exothermic peak can
250 be observed at ~85°C in water which appears to become more pronounced in the presence

of electrolyte. The removal of pyruvate groups from the end of the side chains is expected to facilitate formation of the ordered structure since it reduces electrostatic repulsions and hence the conformational transition shifts to higher temperatures.

Xanthan / KM mixed systems in the absence of electrolyte

The DSC cooling curves for native xanthan and deacetylated xanthan in the presence of konjac glucomannan (1:1 mixing ratio; 1.2% total polysaccharide w/w) are given in Figure 5. The native xanthan / konjac glucomannan (curve a) and deacetylated xanthan / konjac glucomannan (curve b) show a single peak with onset temperatures of 64°C and 59°C respectively. The corresponding G' and G" values of these systems were measured at 1Hz on cooling over the same temperature range and the results are presented in Figure 6. G' is seen to increase at ~64°C and 59°C for the native xanthan and deacetylated xanthan respectively. These temperatures correspond closely with the onset temperature of the conformational transition of the respective samples (Figure 5). The implication is that konjac glucomannan molecules associate strongly with the xanthan molecules once the ordering process has started resulting in the formation of a three dimensional gel structure as reported previously (Annable, Williams & Nishinari 1991). Our key observation is that for these systems, in the absence of electrolyte, the coil-helix transition is the trigger for the interaction to occur. This contradicts the work of Cairns, Miles & Morris (1986) and Brownsey et al (1988) who indicated that binding occurred only with disordered xanthan chains and also with Goycoolea et al (1995) who argued that the interaction can occur with both ordered and disordered chains. Our results indicate that the mechanism of interaction is similar to that for mixtures of konjac glucomannan with kappa carrageenan (Williams et al, 1995) in which molecular association and gelation occur only once the carrageenan molecules form the ordered helical structure. We have demonstrated previously by ESR nitroxide spin labelling studies that the segmental motion of the konjac glucomannan molecules decreases

277 dramatically as the xanthan molecules form the ordered structure and this can only be
278 attributed to association of the konjac glucomannan with xanthan molecules (Annable,
279 Williams & Nishinari, 1994). The values of G' at 20°C and at 1Hz are 1600 Nm^{-2} and 1000
280 Nm^{-2} for the deacetylated and unmodified xanthan samples respectively. Other workers,
281 (Abbaszadeh & Foster, 2012: Tako, Asato & Nakamura, 1984: Shatwell, Sutherland, Ross-
282 Murphy & Dea, 1991) have also reported higher G' values for deacetylated xanthan.

283 The DSC cooling curves for depyruvated xanthan / konjac glucomannan (1:1 mixing ratio;
284 1.2% total polysaccharide w/w) are also presented in Figure 5 curve (c). For this sample two
285 peaks were observed one with an onset temperature at 85°C and the other at 45°C. The
286 corresponding G' and G" values of this system were measured at 1Hz on cooling over the
287 same temperature range and the results are also presented in Figure 6. G' is seen to
288 increase at ~ 45°C although the maximum value attained is considerably lower than for the
289 xanthan and deacetylated xanthan systems. The high temperature DSC peak is attributed to
290 the ordering of the xanthan chains while the peak at lower temperature corresponds to the
291 temperature of gelation. In the case of depyruvated xanthan, the molecules are already
292 ordered at the start of the rheological measurements (75°C) and molecular association with
293 konjac glucomannan molecules occurs at a lower temperature.

294 The ΔH values for the DSC peaks were found to be -8.4 J/g, -11.3 J/g and -2.6 J/g
295 respectively for the native xanthan, deacetylated xanthan and depyruvated xanthan mixtures
296 respectively (Table 2). These values are considerably higher than for the respective xanthan
297 samples alone supporting the concept that konjac glucomannan associates with the xanthan
298 molecules promoting the formation of the ordered structure which leads to the formation of a
299 three dimensional gel network. It is noteworthy that the enthalpy value is highest for the
300 deacetylated sample which is expected to have the least ordered helical structure and lowest
301 for the depyruvated sample which is expected to have the most ordered helical structure.

302

Xanthan / KM mixed systems in the presence of electrolyte

The DSC cooling curves and corresponding G' and G" values at 1Hz for native xanthan / konjac glucomannan mixtures (1:1 mixing ratio; 1.2% total polysaccharide) at varying ionic strength are given in Figures 7 and 8. In the absence of electrolyte a single large exothermic peak is observed by DSC with an onset temperature of ~64°C corresponding to the gelation temperature as noted by the increase in G' (Figure 8). In the presence of 10mM NaCl a similar peak is observed with an onset temperature of 64°C again corresponding to the temperature of gelation (Figure 8). There is also a small DSC peak with an onset temperature at ~47°C. As the ionic strength is increased further to 20mM, 30mM and 40mM NaCl (curves c, d and e) two exothermic peaks are observed by DSC. The enthalpies for all of the peaks are given in Table 2. The peaks at higher temperature have onset temperatures of 70-85°C similar to the peaks observed previously for the xanthan alone. We, therefore, attribute these peaks to the xanthan conformational transition. The peaks at lower temperatures have onset temperatures at ~52°C which corresponds to the gelation temperatures as noted by the increase in G' (Figure 8). It is evident that the value of G' decreases in the presence of electrolyte from 1000 Nm^{-2} in water to 350 Nm^{-2} in 40mM NaCl. The lower value for G' and the lower enthalpy values associated with this peak are indicative of a less extensive interaction between the xanthan and konjac glucomannan molecules.

Similar experiments were undertaken using deacetylated xanthan and the DSC cooling curves and enthalpy values are given in Figure 9 and Table 2 and the corresponding G' and G" values are presented in Figure 10. For the systems in water and 10mM NaCl a large exothermic DSC peak is observed with an onset temperature of ~60°C which corresponds to the temperature of gelation. In the presence of 20mM NaCl (curve c) two exothermic peaks are observed. The peak with Tm at 57°C has a shoulder on the high temperature side which has the same onset temperature as for the conformational transition of deacetylated xanthan itself (Figure 2). The peak corresponds to the temperature of gelation as noted by the increase in the value of G' at ~60°C as shown in Figure 10. The lower temperature peak with

330 a Tm ~50°C is also due to molecular aggregation as noted by a shoulder in the plot of G'
331 against temperature. In the presence of 30 and 40mM NaCl two peaks are observed. The
332 higher temperature peak corresponds to the xanthan conformational transition as reported
333 above (Figure 2) while the lower temperature peak with an onset temperature of 54°C
334 corresponds to the increase in G' as a result of xanthan / konjac glucomannan molecular
335 association. The value of G' decreases from 1600 Nm^{-2} in water to 250 Nm^{-2} in the presence
336 of 40mM NaCl. The lower G' values and lower enthalpies obtained in the presence of
337 electrolyte are again indicative of a less extensive interaction between the deacetylated
338 xanthan and konjac glucomannan molecules.

339 The DSC cooling curves, enthalpy values and corresponding G' and G" values for
340 depyruvated xanthan / konjac glucomannan mixtures in water and 40mM NaCl (1:1 mixing
341 ratio; 1.2% total polysaccharide) are shown in Table 2 and Figures 11 and 12. The DSC
342 cooling curve in water (Figure 11 curve a) shows a small exothermic peak with Tm ~80°C
343 which corresponds to the xanthan conformational transition and a second peak with an onset
344 temperature of~45°C. This lower temperature peak corresponds to gelation as noted by the
345 increase in G' (Figure 12). In the presence of 40mM NaCl (Figure 11 curve b) there is only
346 one peak observed. It is expected that the peak due to the xanthan conformational transition
347 is >90 °C and that the peak observed with an onset temperature of ~50°C corresponds to the
348 increase in G' and the onset of gelation (Figure 12). For depyruvated xanthan the values for
349 G' are very much less than for the standard and deacetylated xanthan samples and contrary
350 to these samples G' increases slightly in the presence of electrolyte. In water at 20C, G' has
351 a value of 210 Nm^{-2} while in 40mM NaCl it increases to 240Nm^{-2}.

352

353 **Conclusions**

354 In summary it is noted that xanthan gum forms thermoreversible gels with konjac
355 glucomannan as a result of molecular association. The gels are stronger in water than in the

356 presence of electrolyte and gel strength decreases in the order deacetylated xanthan /
357 konjac glucomannan > xanthan / konjac glucomannan >>depyruvated xanthan / konjac
358 glucomannan.

359 For native xanthan and deacetylated xanthan mixtures with konjac glucomannan in water the
360 xanthan conformational transition and gelation are coincidental. It appears that as the
361 xanthan molecules order they associate with konjac glucomannan molecules resulting in the
362 formation of a three dimensional gel network. The significantly higher enthalpies obtained for
363 the mixed systems demonstrate that the degree of molecular ordering is greater than for
364 xanthan alone. In addition, the degree of ordering is less for deacetylated xanthan than
365 native xanthan in the absence of konjac glucomannan and it is interesting to note that this
366 results in the deacetylated xanthan having higher enthalpy and G' values indicating
367 increased association between xanthan and konjac glucomannan molecules.

368 For native xanthan and deacetylated xanthan in the presence of electrolyte (>20mM) the
369 xanthan molecules undergo a coil-helix transition at higher temperatures than in water but
370 interaction with konjac glucomannan molecules only occurs at much lower temperatures.
371 This is presumably due to the increased thermal energy of the molecules at high
372 temperature which inhibits molecular association. As the temperature decreases, xanthan /
373 konjac glucomannan association and gelation occurs but to a lesser extent than in the
374 absence of electrolyte as indicated by the lower enthalpies and G' values. We conclude that
375 in these systems self-association of xanthan molecules competes with xanthan / konjac
376 glucomannan association due to charge screening by the electrolyte present.

377 The depyruvated xanthan forms an ordered structure at high temperatures even in the
378 absence of electrolyte and association with konjac glucomannan molecules is much less
379 than for standard and deacetylated xanthan as confirmed by the DSC and rheological
380 measurements.

381

382 **References**

383 Abbaszadeh, A. & Foster, T.J., (2012) 'Effect of Polymer Fine Structure on Synergistic
384 Interactions of Xanthan with Konjac Glucomannan' In *Gums and Stabilisers for the Food*
385 *Industry 16;* Williams, P.A.; Phillips, G.O., Eds.; RSC Publishing, Cambridge, UK, Special
386 Publication No. 335 p 151

387 Annable, P., Williams, P.A. & Nishinari, K., Interaction in xanthan – glucomannan mixtures
388 and the effect of electrolyte (1994) *Macromolecules* 27, 4204

389 Brownsey, G.J., Cairns, P., Miles, M.J.& Morris, V.J., Evidence for intermolecular binding
390 between xanthan and the glucomannan konjac mannan (1988) *Carbohydrate Res*earch 176,
391 329

392 Cairns, P., Miles, M.J. & Morris, V.J., Intermolecular bonding of xanthan gum and carob gum
393 (1986) 322, 89-90

394 Callet, F., Milas, M. & Rinaudo, M., Influence of acetyl and pyruvate contents on rheological
395 properties of xanthan in dilute solution (1987) *International Journal of Biological*
396 *Macromolecules* 9, 291-293

397 Cheetham. N.W.H. & Mashimba, E. N.M., Conformational aspects of xanthan-
398 galactomannan gelation. Further evidence from optical –rotation studies (1992)
399 *Carbohydrate Polymers* 14, 17

400 Dea, I.C.M., Morris, E.R., Rees, D.A., Welsh, E.J., Barnes, H.A. & Price, J. Associations of
401 like and unlike polysaccharides: Mechanism and specificity in galctomannans, interacting
402 bacterial polysaccharides, and related systems (1977) *Carbohydrate Research* 57, 249-272

403 Dea, I.C.M. & Morrison, A., Chemistry and interaction of seed galactomannans (1975)
404 *Advances in Carbohydrate Chemistry and Biochemistry* 31, 241

405 Fitzsimons, S. M., Tobin, J.T. & Morris, E.R., Synergistic binding of konjac glucomannan to
406 xanthan on mixing at room temperature (2008) *Food Hydrocolloids* 22 36-46

407 Foss, P., Stokke, B.T. & Smidsrød, O., Thermal stability and chain conformational studies of
408 xanthan at different ionic strengths (1987) *Carbohydrate Polymers,* 7, 421-433

409 Gamini, A., de Bleijser, J. & Leyte, J.C., Physico-chemical properties of aqueous solutions of
410 xanthan: An nmr study (1991) *Carbohydrate Research*, 220, 33-47

411 Goycoolea, F.M., Richardson, R.K., Morris, E.R. & Gidley, M.J. Stoichiometry and
412 conformation of xanthan in synergistic gels with locust bean gum or konjac glucomannan:
413 Evidence of heterotypic binding, Macromolecules (1995) 28, 8308-8320

414 Kitamura, S., Takeo, K., Kuge, T.& Stokke, B.T. Thermally induced conformational transition
415 of double stranded xanthan in aqueous solution (1991) *Biopolymers* 31, 1243-55

416 Lui, W. & Norisuye, T., Thermally induced conformational change of xanthan: interpretation
417 of viscosity behaviour in 0.01M aqueous sodium chloride (1988) *International Journal of*
418 *Biological Macromolecules* 10, 44

419 Manning, G.S., Limiting laws and counterion condensation in polyelectrolyte solutions I
420 Colligative properties (1969a) *Journal Chemical Physics* 51, 924-933

421 Manning, G.S., Limiting laws and counterion condensation in poplyelectrolyte solutions III An
422 analysis based on Mayer ionic solution theory (1969b) *Journal Chemical Physics* 51, 3249-
423 3252

424 Manning,G.S. Critical onset counterion condensation. A survey if its experimental and
425 theoretical basis (1996) *Ber. Bunsen-Ges. Phys. Chem.* 100, 909-922,

426 Milas, M. & Rinaudo, M., Properties of xanthan gum in aqueous solutions: role of the
427 conformational transition (1986) *Carbohydrate Research* 158, 191

428 Moorhouse, R., Walkinshaw, M.D.& Arnott, S., (1977) *ACS Symposium Series*
429 45, 90-102
430 Morris, V.J. Bacterial polysaccharides (2006) In *Food Polysaccharides and Their*
431 *Applications 2nd edition* Stephen, A.M.; Phillips, G.O.; Williams, P.A., Eds,; CRC Press,
432 Taylor and Francis Group, Boca Raton, Fl, USA pp413-454

433 Nishinari, K., Williams, P.A. & Phillips, G.O. Review of the physicochemical characteristics
434 and properties of konjac mannan (1992) *Food Hydrocolloids 6,* 199-222

435 Norton, I.T., Goodall, D.M., Frangou, S.A., Morris, E.R. & Rees, D.A., Mechanism and
436 dynamics of conformational ordering in xanthan polysaccharide (1984) *Journal of Molecular*
437 *Biol*ogy 175, 371-394

438 Shatwell, K.P., Sutherland, I.W., Dea, I.C.M. & Ross-Murphy, S.B. The influence of acetyl
439 and pyruvate substituents on the coil-helix transition behaviour of xanthan (1990)
440 *Carbohydrate Research 206,* 87-103

441 Shatwell, K.P., Sutherland, I.W., Ross-Murphy, S.B. Dea, I.C.M., Influence of the acetyl
442 substituent on the interaction of xanthan with plant polysaccharides – III. Xanthan – konjac
443 mannan systems (1991) *Carbohydrate Polymers* 14, 131-147

444 Sloneker, J.H.& Orentas, D.G., Pyruvic acid, a unique component of an exocellular bacterial
445 polysaccharide (1962) *Nature* 194, 478-479

446 Sworn, G., (2009) Xanthan gum. In *Handbook of hydrocolloids 2nd edition* Phillips, G.O.;
447 Williams, P.A. Eds.; CRC Press, Woodhead Publishing Ltd, Cambridge, UK, p 186

448 Tako, M., Asato, A. & Nakamura, S., Rheological aspects of the intermolecular interaction
449 between xanthan and locust bean gum in aqueous media (1984) *Agricultural and Biological*
450 *Chemistry* 12, 2995-3000

451 Tako, M. & Nakamura, S., Rheological properties of deacetylated xanthan in aqueous
452 solution (1984) *Agricultural and Biological Chem*istry 48, 2987-2993

453 Takigami, S., (2009) Konjac mannan In *Handbook of hydrocolloids 2nd edition* Phillips, G.O.;
454 Williams, P.A. Eds.; CRC Press, Woodhead Publishing Ltd, Cambridge, UK, p 889

455 Takigami, S., Shimada, M., Williams, P.A.; & Phillips, G.O., ESR study of the conformational
456 transition of spin-labelled xanthan gum in aqueous solution (1993) *International Journal of*
457 *Biological Macromol*ecules 15, 367-371

458 Velez, G., Fernandez, M.A., Munoz J. & Williams, P.A., English R.J. (2003) The
459 role of hydrocolloids on the creaming of oil-in-water emulsions *Journal of*
460 *Agricultural & Food Chemistry* 51, 265-269
461 Wielinga, W.C., (2009) Galactomannans, In *Handbook of hydrocolloids 2nd edition* Phillips,
462 G.O.; Williams, P.A. Eds.; CRC Press, Woodhead Publishing Ltd, Cambridge, UK, p 228

463 Williams, P.A., Clegg, S.M., Day, D.H., Phillips, G.O. & Nishinari, K., (1991a) Mixed gels
464 formed with konjac mannan and xanthan gum, In *Food Polymers, Gels and Colloids,*
465 Dickinson, E. Ed. RSC Special Publication N0. 82 Cambridge p 339

466 Williams, P. A.; Clegg, S. M.; Langdon, M. J.; Nishinari, K.; Piculell L.,
467 Investigation of kappa carrageenan / konjac mannan mixed gels by differential
468 scanning calorimetry and electron spin resonance spectroscopy (1993)
469 *Macromolecules* 26, 5441-5446

470 Williams, P.A., Day, D.H., Langdon, M.J., Phillips, G.O. Nishinari, K., Synergistic interaction
471 of xanthan with gluco- and galacto- mannans (1991b) *Food Hydrocollolloids* 4, 489-493

472 Williams, P.A. & Phillips, G.O., (1995) Interactions In Mixed Polysaccharide Systems, In
473 *Food Polysaccharides and Their Applications*; Stephen, A.M., Ed.; Marcel Dekker Inc.: New
474 York, p 463

475 **List of Figures**

498 Figure 11 DSC cooling curves for depyruvated xanthan / KM solutions (1:1 mixture; 1.2%
499 total polysaccharide) in (a) water and (b) 40mM NaCl

500 Figure 12 Variation of G' and G" at 1Hx on cooling for depyruvated xanthan / KM mixtures
501 (1:1 mixing ratio; 1.2% total polysaccharide) in water and 40mM NaCl

502
503
504
505
506
507
508
509
510
511

512 **Figure 1 DSC cooling curves for 1.2% native xanthan gum solution in (a) water (b)**
513 **5mM (c) 8mM (d) 10mM (e) 20mM (f) 30mM and (g) 40 mM NaCl**

514

515

516

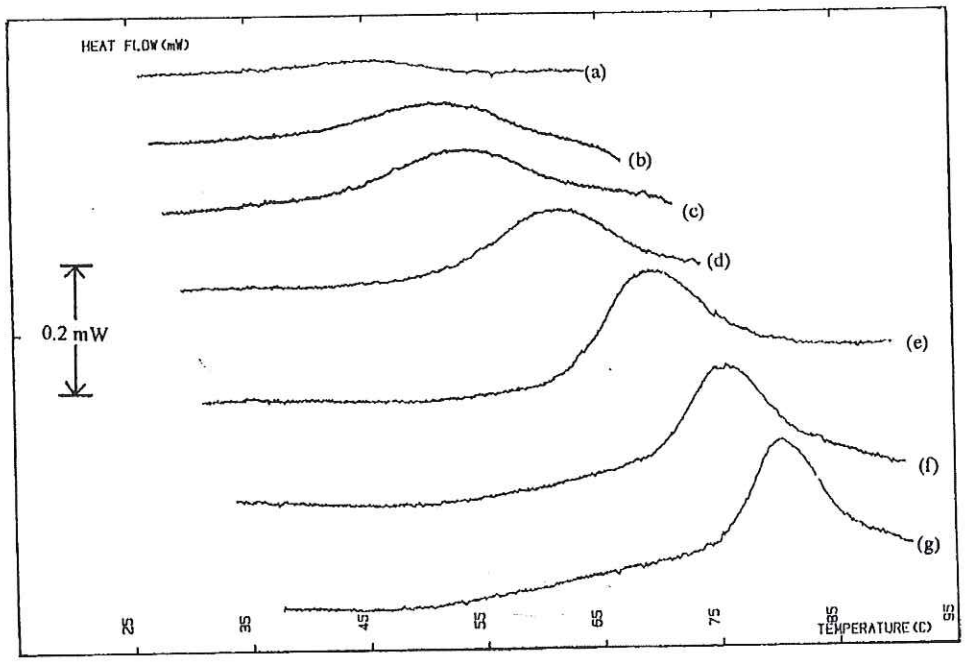

517

518

519 **Figure 2 DSC cooling curves for deacetylated xanthan gum (1.2%) in (a) water (b)**
520 **10mM (c) 20mM (d) 30mM and (e) 40 mM NaCl**

521

522

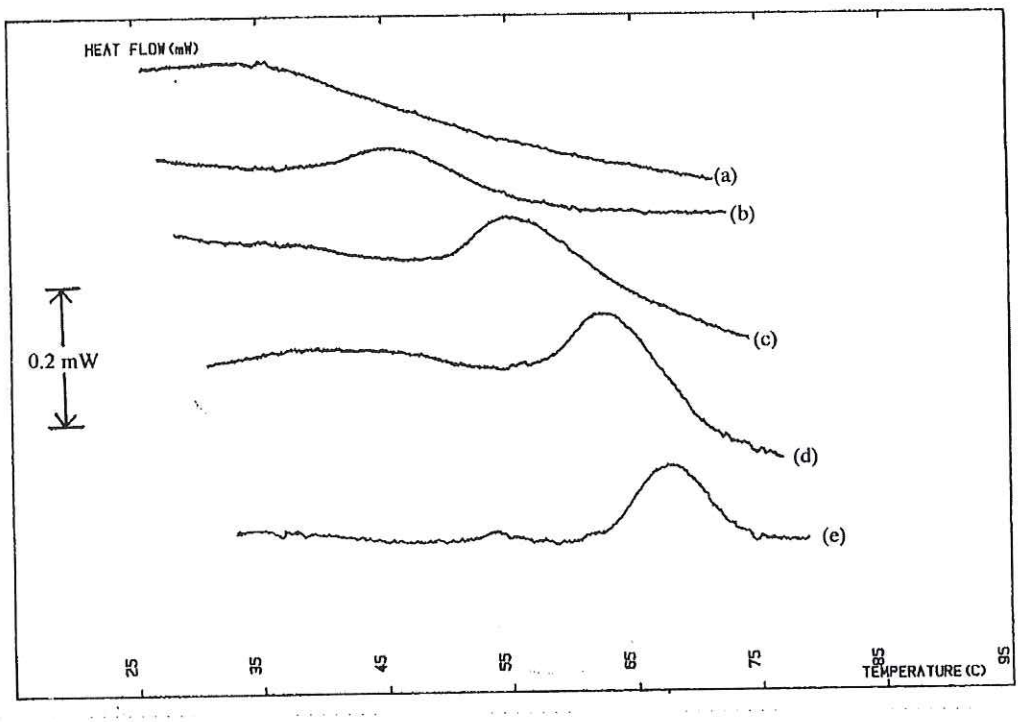

523

524

525

526

527

528

529

530

531

532

533

534

535

536

Figure 3 Plot of the inverse of the midpoint transition temperature with the natural log of the ionic strength for native xanthan gum, deacetylated xanthan gum and depyruvated xanthan gum solutions

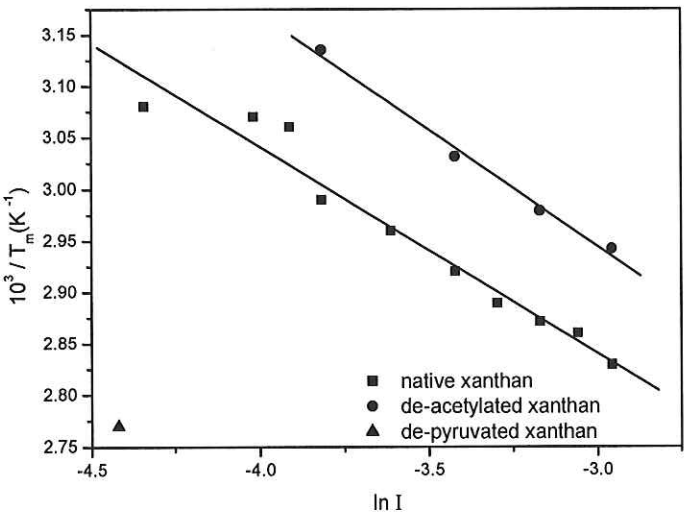

549 **Figure 4 DSC cooling curves for depyruvated xanthan (1.2% w/w) in (a) water and (b)**
550 **40mM NaCl**

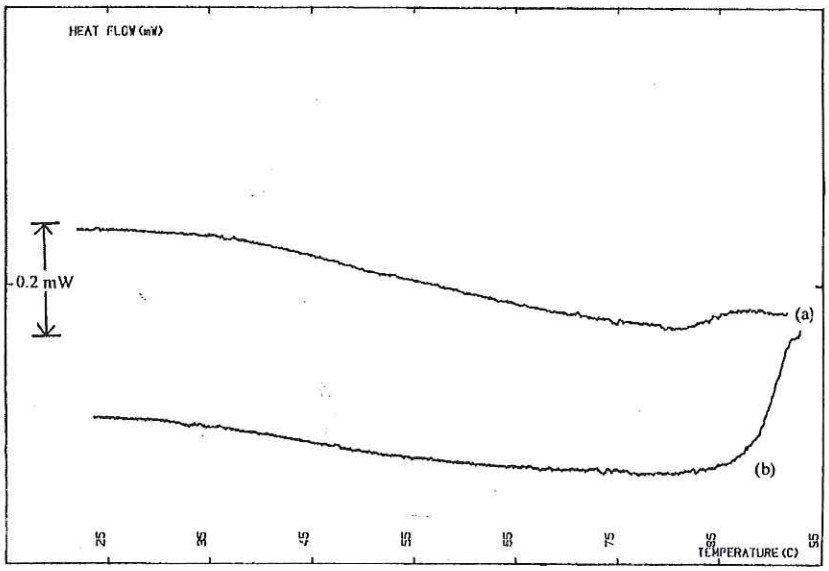

551

552 **Figure 5 DSC cooling curves for (a) native xanthan gum (b) deacetylated xanthan gum**
553 **and (c) depyruvated xanthan in admixture with KM (1:1 mixing ratio; 1.2% total**
554 **polysaccharide)**

555

556

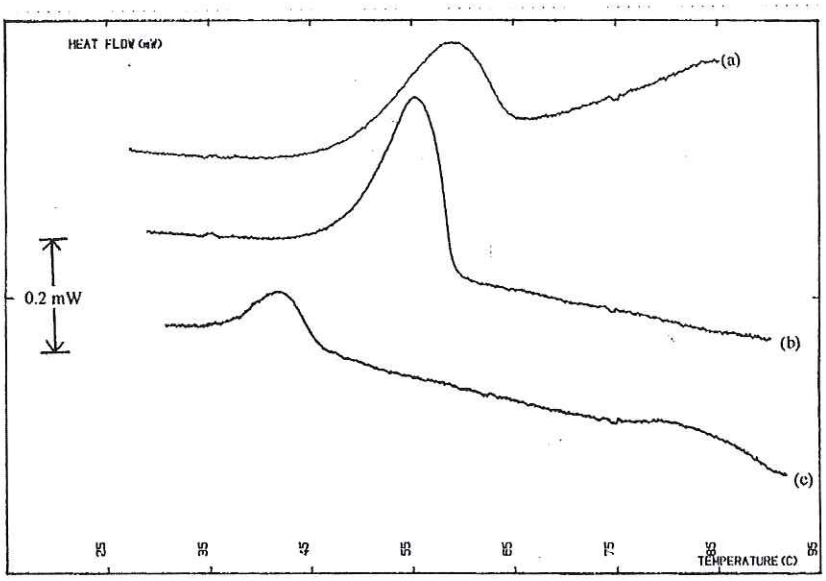

557

558 **Figure 6 Variation of G' and G" at 1Hz of native xanthan / KM samples [mixing ratio**
559 **1:1; 1.2% total polysaccharide] on cooling**

560

561

562

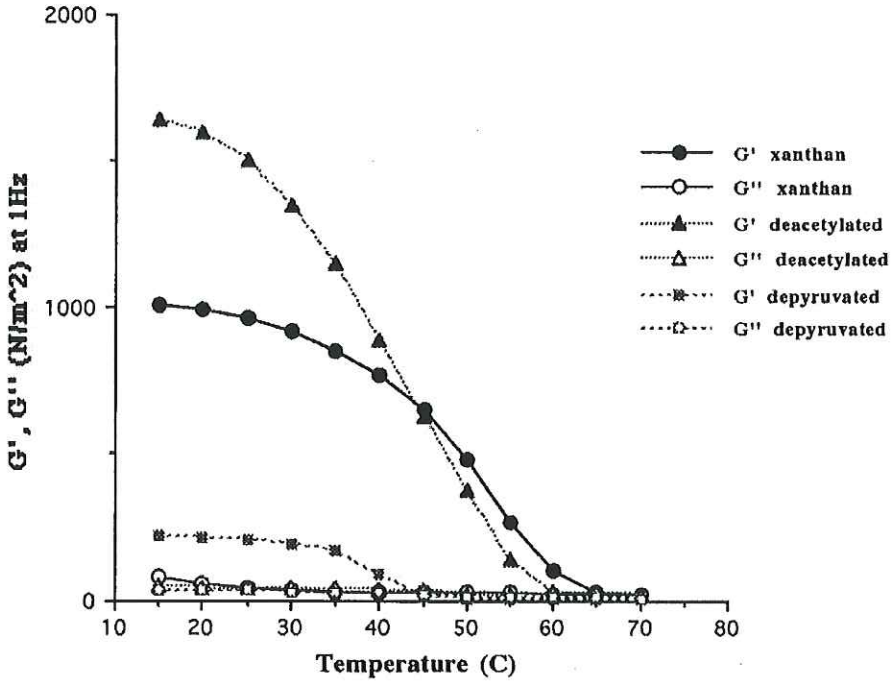

563

564

Figure 7 DSC cooling curves for native xanthan gum / KM solutions (1:1 mixing ratio; 1.2% total polysaccharide) in (a) water (b) 10mM (c) 20mM (d) 30mM (e) 40mM NaCl. The arrow denotes the temperature of gelation.

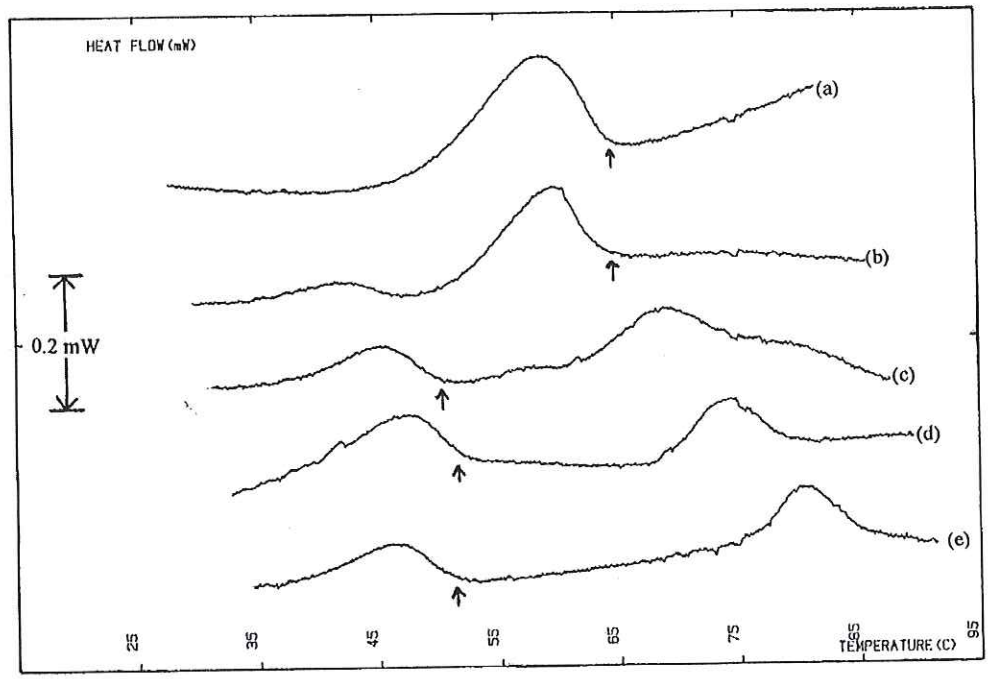

573 **Figure 8 Variation of G' and G" at 1Hz on cooling for native xanthan gum / KM**
574 **solutions (1:1 mixing ratio; 1.2% total polysaccharide) at different ionic strengths**

575

576

577

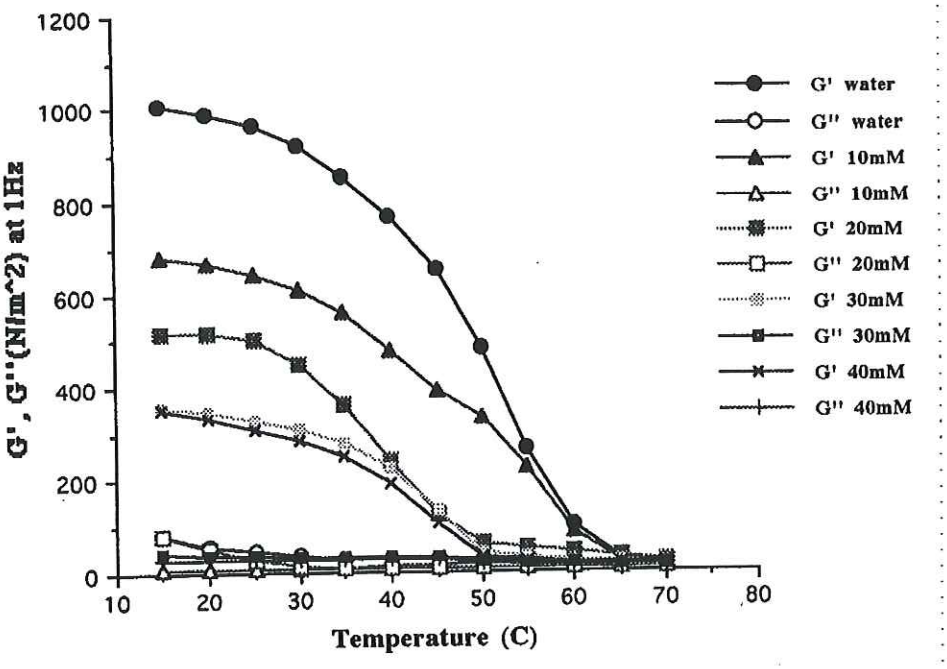

578

579

580

581

582 **Figure 9 DSC cooling curves for deacetylated xanthan / KM (1:1 mixture: total**
583 **polysaccharide concentration 1.2%) in (a) water (b) 10mM (c) 20mM (d) 30mM (e) 40**
584 **mM NaCl. The arrow denotes the temperature of gelation**

585

586

587

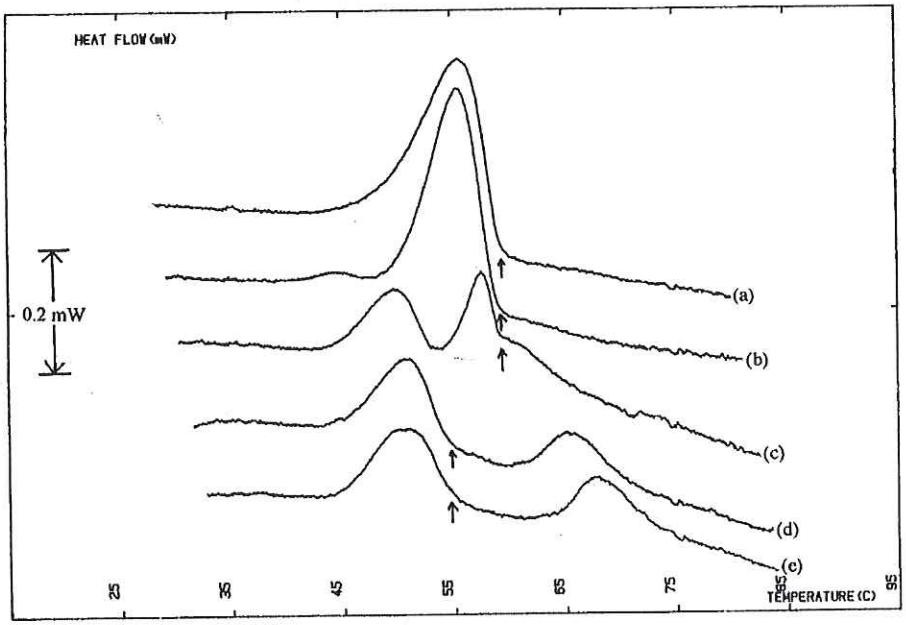

588

589 **Figure 10 Variation of G' and G" at 1Hz on cooling for deacetylated xanthan / KM (1:1**
590 **mixing ratio, 1.2% total polysaccharide concentration at different ionic strengths**

591

592

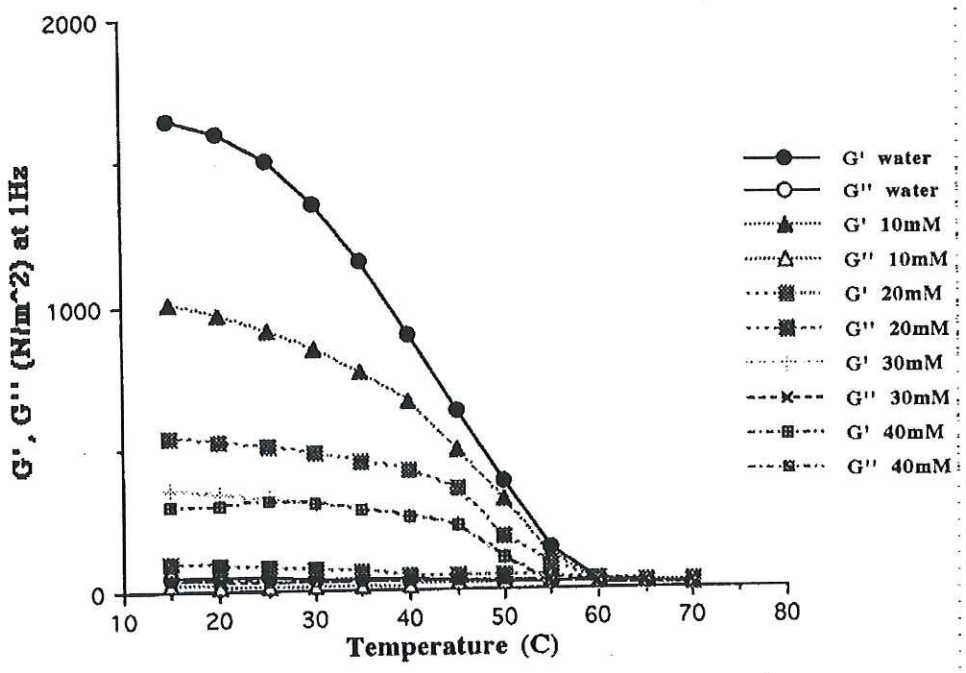

593

594

Figure 11 DSC cooling curves for depyruvated xanthan / KM solutions (1:1 mixture; 1.2% total polysaccharide) in (a) water and (b) 40mM NaCl

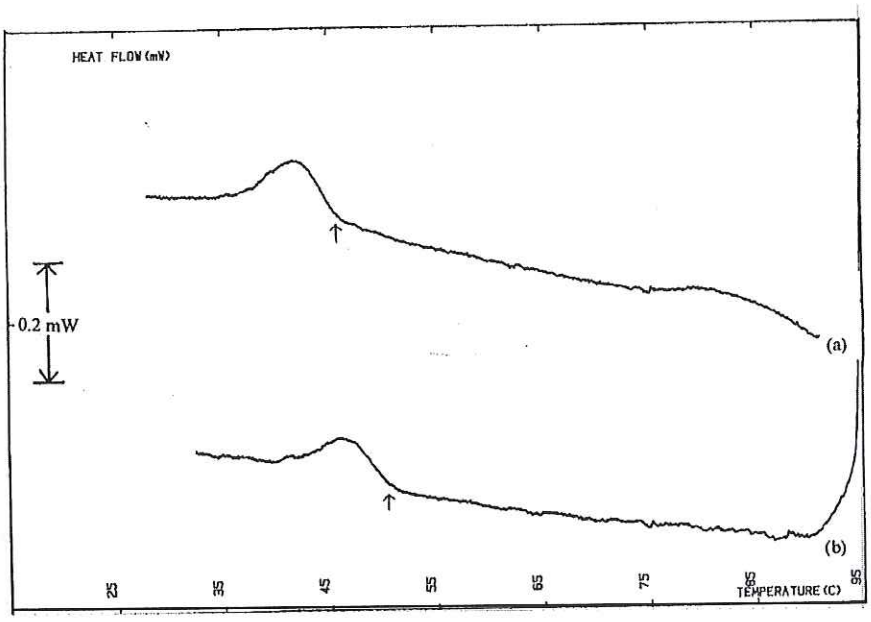

615 **Figure 12 Variation of G' and G" at 1Hz on cooling for depyruvated xanthan / KM**
616 **mixtures (1:1 mixing ratio; 1.2% total polysaccharide) in water and 40mM NaCl**

617

618

619

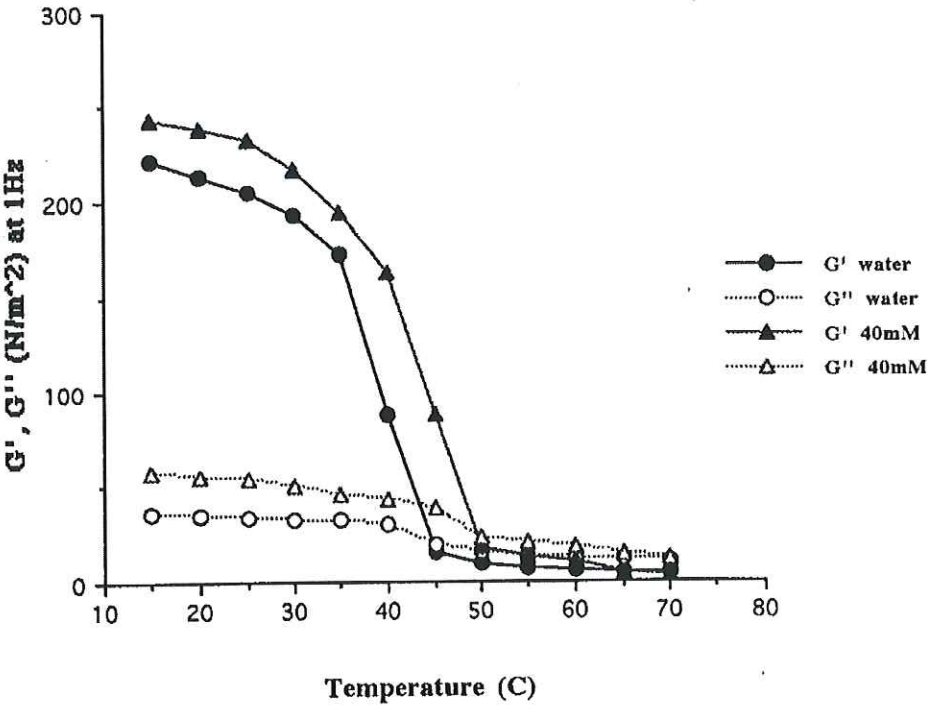

620

621

622 **Table 1 Enthalpy and transition midpoint temperatures as a function of ionic strength**
623 **for native xanthan and deacetylated xanthan on cooling**

624

Ionic strength / mM	Native xanthan		Deacetylated xanthan	
	Tm	ΔH / J/g	Tm	ΔH / J/g
1	51.4	-2.6		
5	52.1	-2.7		
8	53.7	-3.3		
10	61.0	-5.2	45.8	-2.5
15	65.2	-5.6		
20	69.1	-6.6	56.7	-4.2
25	73.0	-6.5		
30	75.2	-6.3	62.6	-4.1
35	76.5	-6.5		
40	80.3	-6.5	66.8	-4.0

625

626

627

628

629 **Table 2 Enthalpy and onset temperatures as a function of ionic strength for natuve**
630 **xanthan, deacetylated xanthan and depyruvated xanthan in admixture with KM on**
631 **cooling**

Ionic strength / mM	Native xanthan/KM ΔH J/g		Deacetylated xanthan/KM ΔH J/g		Depyruvated xanthan/KM ΔH J/g	
	Peak onset ~64 °C	Peak onset ~50 °C	Peak onset ~ 59 °C	Peak onset ~ 54 °C	Peak onset ~ 50 °C	Peak onset ~ 45 °C
Water	-8.38		-11.28			-2.63
10	-4.67	-0.79	-10.79			
20		-2.12	-2.60	-2.52		
30		-2.88		-4.38		
40		-2.25		-4.43	-2.13	

632